Bulk Growth and Characterization of a Novel Nonlinear Optical Crystal BaTeMo2O9

ARTICLE *in* CRYSTAL GROWTH & DESIGN · DECEMBER 2007

Impact Factor: 4.89 · DOI: 10.1021/cg700755p

CRYSTAL GROWTH & DESIGN
2008
VOL. 8, NO. 1
304–307

Bulk Growth and Characterization of a Novel Nonlinear Optical Crystal $BaTeMo_2O_9$

Weiguo Zhang, Xutang Tao,* Chengqian Zhang, Zeliang Gao, Yongzhuan Zhang, Wentao Yu, Xiufeng Cheng, Xuesong Liu, and Minhua Jiang

State Key Laboratory of Crystal Materials, Shandong University, Jinan, 250100, P. R. China

Received August 9, 2007; Revised Manuscript Received September 27, 2007

ABSTRACT: A new nonlinear optical crystal $BaTeMo_2O_9$ was grown from the TeO_2-MoO_3 flux system with sufficient size ($30 \times 23 \times 18$ mm^3) and optical quality that allowed the characterization of its properties. It crystallizes in the noncentrosymmetrical system, space group $P2_1$ (no. 4), with $a = 5.5346$ Å, $b = 7.4562$ Å, $c = 8.8342$ Å, and $\beta = 90.897°$. The as-grown $BaTeMo_2O_9$ crystal has well-developed faces with the major forms {100}, {001}, {011}, and {01$\bar{1}$}. The transmission spectra results suggest that it can transmit well from 0.5 to 5.0 μm. The refractive indices were also measured. The smaller refractive indices n_x and n_y are in the *ac*-plane, and the largest refractive index n_z polarization direction is parallel to the crystallographic *b*-axis.

Introduction

Noncentrosymmetric (NCS) compounds are of current interest owing to their properties such as ferroelectricity, piezoelectricity, dielectric behavior, and second-order nonlinear optical (NLO) phenomena. Especially nonlinear optical phenomena exhibit excellent applications such as frequency shifting, optical modulating, and telecommunications and signal processing. Recently, a variety of strategies have been put forth for creating new NCS materials by synthesizing compounds with d^0 transition metal cations (Mo^{6+} or W^{6+}) and cations with nonbonded electron pairs (Se^{4+} or Te^{4+}).[1–13] Both kinds of ions are susceptible to the second-order Jahn–Teller (SOJT) effect, and the influence of a SOJT distortion on the NCS structure was reported by Halasyamani et al.[14] These materials show relatively large powder second-harmonic generation (SHG) efficiencies such as $Na_2TeW_2O_9$ 500 × α-SiO_2,[8] $Rb_2TeW_3O_{12}$ 200 × α-SiO_2[10] $Cs_2TeW_3O_{12}$ 400 × α-SiO_2,[10] $BaTeW_2O_9$ 500 × α-SiO_2[11] and $Na_2Te_3Mo_3O_{16}$ 500 × α-SiO_2.[13] The noteworthy compound $BaTeMo_2O_9$ is one of these materials and was first synthesized by Ra et al. through the traditional solid-state reaction method and, its powder SHG efficiency is about 600 × α-SiO_2.[11] It is also known that in octahedrally coordinated d^0 transition metal oxides,[15] the average distortion scale is as follows: $Mo^{6+} \approx V^{5+} >> W^{6+} \approx Ti^{4+} \approx Nb^{5+} > Ta^{5+} >> Zr^{4+} \approx Hf^{4+}$. Among these new NCS materials, $BaTeMo_2O_9$ has the strongest powder SHG efficiency. However, until now, all the studies on these materials have been limited to the synthesis and measurement of powders. The crystal growth and characterization of these new NCS materials with technological importance have not been reported before.

In this paper, we report the bulk growth of a $BaTeMo_2O_9$ single crystal in detail for the first time by the flux method. We have also studied the morphology and properties such as the X-ray powder diffraction, single-crystal X-ray diffraction, transmission spectra, and refractive indices of the crystal.

Experimental Section

Syntheses of Polycrystalline $BaTeMo_2O_9$. Polycrystalline $BaTeMo_2O_9$ was synthesized by solid-state reaction techniques. Stoichiometric amounts of $BaCO_3$, TeO_2, and MoO_3 ($BaCO_3$:TeO_2:MoO_3 molar ratio = 1:1:2) were ground and packed into columns and heated to 500 °C for 20 h, 520 °C for 20 h, and 550 °C for 20 h orderly with intermittent regrindings. In this way, white products were obtained. XRD investigations on polycrystalline $BaTeMo_2O_9$ were carried out with a Bruker D8 advanced diffractometer equipped with Cu Kα radiation ($\lambda = 1.54056$ Å). The data were collected using a Ni-filtered Cu-target tube at room temperature in the 2θ range from 10° to 70°.

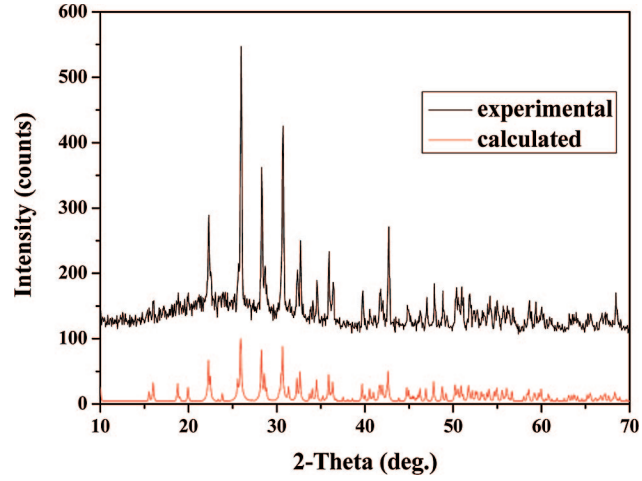

Figure 1. Calculated and observed powder X-ray diffraction pattern for polycrystalline $BaTeMo_2O_9$.

Growth of the $BaTeMo_2O_9$ Single Crystal. Single crystals of $BaTeMo_2O_9$ were grown from a TeO_2-MoO_3 system by the flux method. Polycrystalline $BaTeMo_2O_9$ (0.2 mol) was poured into the liquid mixture of TeO_2-MoO_3 (0.8 mol each) system at 650 °C in a platinum crucible in a vertical furnace at the constant temperature region followed by stirring for 24 h to form a well-proportioned solution. The furnace temperature was measured by a Pt−Rh thermocouple and controlled by a Shimaden FP23 controller/programmer connected to a thyristor. Another way to prepare the solution is to heat initial reagents of $BaCO_3$, TeO_2, and MoO_3 (at a molar ratio 1:5:6) slowly to 650 °C and stir for 24 h. The seeds of $BaTeMo_2O_9$ were selected from spontaneous nucleation crystals. The saturation temperature was determined by observing the growth or dissolution of crystal seeds on the solution surface. From the saturation temperature, the solution was cooled at a rate of 0.5–1 °C/d. A single crystal was grown on the *a*-axis or *b*-axis oriented seed and rotating at 20–40 rpm placed at the center of the solution surface. Then, the single crystal was hung over the solution surface and cooled slowly to room temperature.

X-ray Diffraction. A block-shaped single crystal with dimensions of $0.11 \times 0.10 \times 0.09$ mm^3 was mounted on glass fiber with epoxy. Single-crystal X-ray diffraction data were collected in the 2θ range

* Corresponding author. E-mail address:txt@icm.sdu.edu.cn.

10.1021/cg700755p CCC: $40.75
Published on Web 12/07/2007

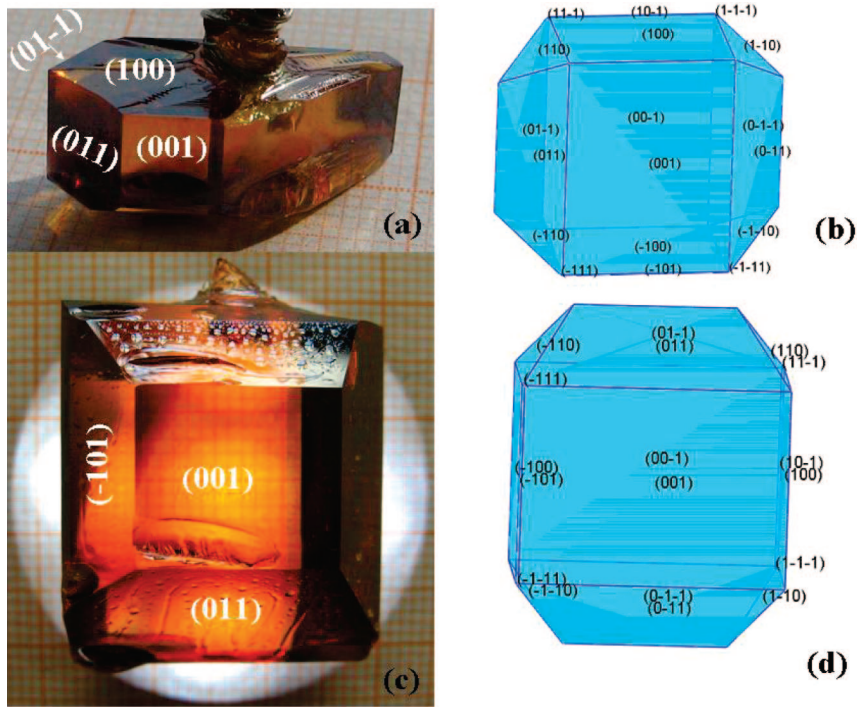

Figure 2. Morphology of obtained (a) *a*-oriented growth and (c) *b*-oriented growth and ideal (b and d) $BaTeMo_2O_9$ crystals.

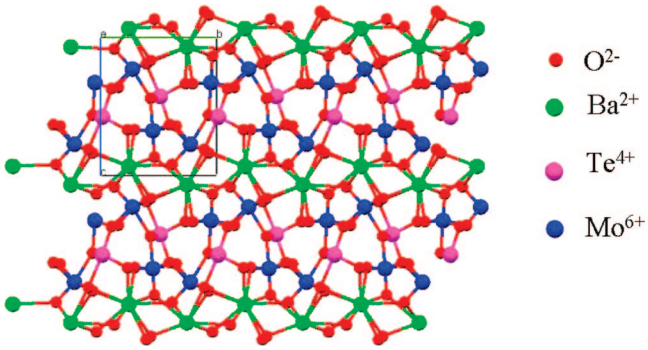

Figure 3. Ball-and-stick diagram of a $BaTeMo_2O_9$ single crystal in the *bc*-plane.

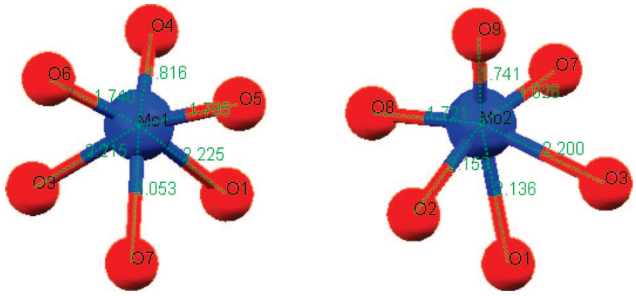

Figure 4. Distances (Å) for Mo(1)−O and Mo(2)−O. Note that Mo^{6+} cations are in asymmetric coordination environments with three short and three long Mo−O bonds, respectively.

from 2.31° to 37.12° using a Bruker APEX2 CCD area-detector diffractometer with graphite monochromated Mo Kα radiation (λ = 0.71073 Å) at 293 K. The structural model was refined using SHELXL-97 (Sheldrick, 1997).

Optical Transmission. Room-temperature optical transmission spectra of the single crystal were measured by a Hitachi U-3500 UV-vis-IR spectrometer and a Nicolet NEXUS 670 FTIR spectrometer.

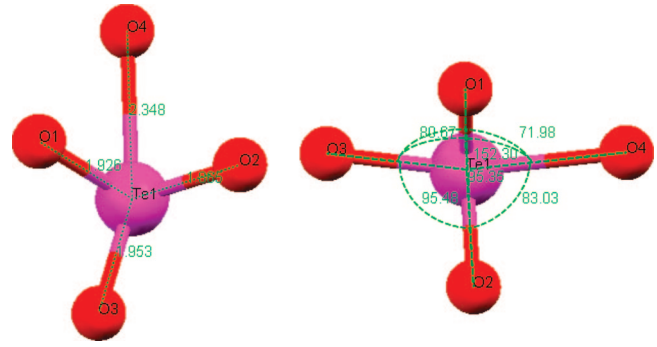

Figure 5. Distances (Å) for the Te−O bonds and angles (deg) for O−Te−O bonds.

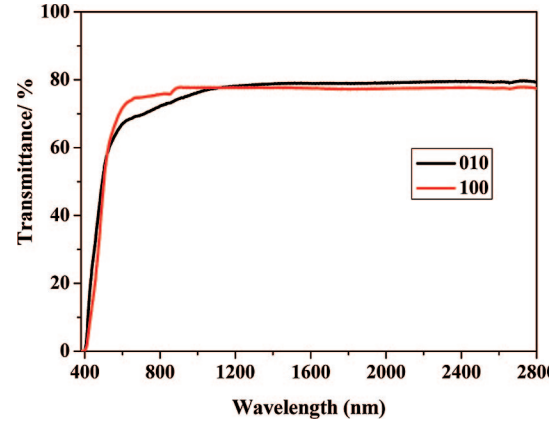

Figure 6. UV-vis-NIR spectra of the $BaTeMo_2O_9$ crystal with the light vertical to the (010) and (100) planes, respectively.

Two 3 and 2 mm thick plate samples of $BaTeMo_2O_9$ were cut and polished respectively for the {010} and {100} forms to do the measurements.

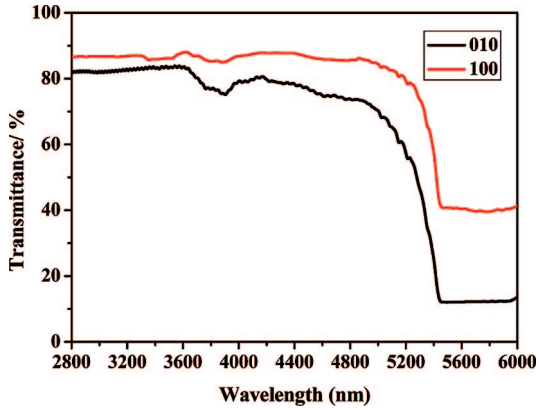

Figure 7. Mid-IR spectra of the $BaTeMo_2O_9$ crystal with the light vertical to the (010) and (100) planes, respectively. Note that there is acceptable transmission even at 5200 nm.

Table 1. Sellmeir Coefficients Derived from the Measured Refractive Indices

Sellmeir coefficients	n_x	n_y	n_z
A	3.93984	4.38509	4.52957
B	0.06606	0.09641	0.11108
C	0.5179	0.07015	0.06523
D	0.0139	0.02796	0.02242

Refractive Index Measurement. The refractive index *n* of $BaTeMo_2O_9$ was measured by using the vertical-incidence method. Several monochromatic sources in the visible and near IR, generated by Hg, H, He, and Na lamps, were used to measure the values of the refractive indices.

Results and Discussion

Synthesis and Characterization of Polycrystalline $BaTeMo_2O_9$. Polycrystalline $BaTeMo_2O_9$ was synthesized by solid-state reaction techniques. Stoichiometric amounts of $BaCO_3$, TeO_2, and MoO_3 ($BaCO_3$:TeO_2:MoO_3 molar ratio = 1:1:2) and homogeneity are both important for the synthesis of pure single phase polycrystalline $BaTeMo_2O_9$. Powder X-ray diffraction patterns of the polycrystalline phases are in good agreement with the calculated pattern derived from the single crystal data. Figure 1 shows the calculated and experimental patterns of powder XRD of polycrystalline $BaTeMo_2O_9$.

Flux Growth and Characteristics of the $BaTeMo_2O_9$ Single Crystal. The flux growth technique is particularly preferable because it readily allows crystal growth at a temperature well below the melting point of the solute. In addition, crystals grown from flux have an enhedral habit and a reasonably lower degree of dislocation density.[16] Well-developed blocklike single crystals of $BaTeMo_2O_9$ were grown from the TeO_2-MoO_3 flux system. Yellow and transparent crystals up to 20 (length) × 10 (width) × 8 (thickness) mm^3 and 30 (length) × 23 (width) × 18 (thickness) mm^3 were obtained with the growth directions of the *a*-axis and *b*-axis oriented seed, respectively. Their sizes were dependent on the solute amount and the growth periods. Figure 2 shows the typical grown and ideal crystal morphology of $BaTeMo_2O_9$.

As shown in Figure 2b (Figure 2d), the ideal morphology of $BaTeMo_2O_9$ deduced from the single-crystal data by the mercury program[17–19] is a polyhedron with four basal, ten sided, and four cornual faces. For the *a*-axis oriented grown $BaTeMo_2O_9$ crystal, the major forms are {100}, {001}, {011}, and {01$\bar{1}$} (Figure 2a). For the *b*-axis oriented grown $BaTeMo_2O_9$ crystal,

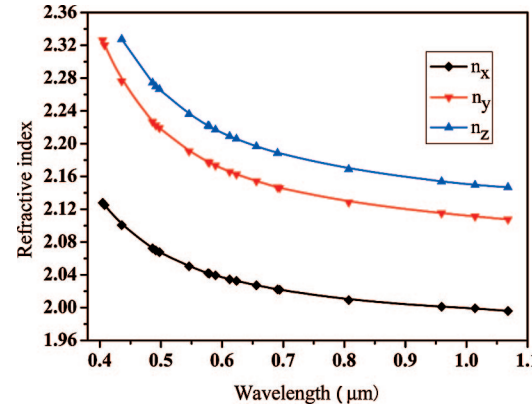

Figure 8. Dispersion of the refractive indices and calculated curves from the Sellmeir coefficients for the $BaTeMo_2O_9$ crystal.

the major forms are {100}, {001}, {011}, {01$\bar{1}$}, {$\bar{1}$01}, and {201} (Figure 2c). From Figures 2a and 2c, we can see that the major faces of the actual $BaTeMo_2O_9$ crystals are very flat. The interfacial angles between basal (1)−basal (2) faces, basal (1)−side (1) faces, basal (1)−side (2) faces, and basal (2)−side (3) faces were respectively 91 ± 0.5°, 50 ± 0.5°, 31 ± 0.5°, and 49 ± 0.5°. These values are in good agreement with the calculated interfacial angles of 90.90° between the (100) and (001) faces, 51.34° between the (100) and (201) faces, 32.10° between the (100) and ($\bar{1}$01) faces, and 49.83° between the (001) and (011) faces, respectively. However, the faces in the ideal crystal appeared to disappear and actually may be attributable to the growth rate and the ratio between polycrystalline $BaTeMo_2O_9$ and the TeO_2-MoO_3 system.

The $BaTeMo_2O_9$ crystal structure has been reported by Ra et al.[11] To reconfirm the crystal structure, single-crystal X-ray diffraction data were collected. The compound crystallizes in a noncentrosymmetric space group, $P2_1$, which is a basic precondition for a potential harmonic generation material. The crystal cell parameters are a = 5.5346 Å, b = 7.4562 Å, c = 8.8342 Å, β = 90.897°, Z = 2, and V = 364.517(9) $Å^3$. The compound has two-dimensional layered structures consisting of MoO_6 octahedra linked to TeO_4 tetrahedra. There are no distinct differences in our work from theirs except for the unit cell parameters and bond distances. The anionic layers are linked by Ba^{2+} cations which also maintain charge balance (Figure 3). The bond distances for Mo(1)−O and Mo(2)−O range from 1.734(2) to 2.225(2) and 1.721(3) to 2.200(2) Å (Figure 4). The Te−O bond distances and O−Te−O angles range from 1.865(2) to 2.347(2) Å and 71.98(8) to 152.30(9)° (Figure 5), respectively. Both the Mo^{6+} and Te^{4+} cations are in asymmetric coordination environments attributable to SOJT distortions.[11]

Optical Properties of the $BaTeMo_2O_9$ Crystal. Figures 6 and 7 show the room-temperature transmission spectra of the $BaTeMo_2O_9$ crystal with the light vertical to the (001) and (010) faces, respectively. The results indicated that the $BaTeMo_2O_9$ crystal presents a good transparency from 0.5 to 5.0 μm, with a weak broad absorption peak around 3.8 μm. Their ultraviolet and infrared absorption edges are at 0.4 and 5.4 μm, respectively.

The refractive indices $n(\lambda)$ of $BaTeMo_2O_9$, as a function of wavelength λ, were measured by using the vertical-incidence method. The accuracy of the measurements is estimated to be 5×10^{-5}, which permits a sufficiently accurate prediction of the phase-matching directions owing to the large birefringence. When monochromatic sources are vertically incident to the (010) plane, two orthorhombic refractive indices n_x and n_y are obtained. Their polarization directions are both in the *ac*-plane.

While monochromatic sources are vertically incident to the (001) plane, another two orthorhombic refractive indices n_z and n_a' are obtained. The refractive index n_z polarization direction is parallel to crystallographic *b*-axis. The dispersion parameters of the refractive index n_i were fitted by the least-squares method according to the Sellmeir equation:[20]

$$n_i^2 = A + \frac{B}{\lambda^2 - C} - D\lambda^2 \quad (1)$$

where λ is the wavelength in micrometers and A, B, C, and D are the Sellmeir parameters. For each refractive index, the four coefficients are listed in Table 1. To verify the obtained results, we calculated the differences between the measured data and the calculated values. The curves obtained from the fit according to this equation and the experimental data are in good agreement, as can be seen in Figure 8. The smaller difference between the values of n_z and n_y than that between the values of n_y and n_x indicated that the $BaTeMo_2O_9$ crystal is an optically negative biaxial crystal.

Conclusions

We have successfully grown bulk $BaTeMo_2O_9$ crystals by the flux method for the first time. The optical characterization of the $BaTeMo_2O_9$ crystal indicates that the crystal transmission region is from 0.4 μm. The refractive indices measurements show that the $BaTeMo_2O_9$ crystal has large values of refractive index and birefringence and is phase-matchable. All the properties indicate its potential application as a new nonlinear optical material.

Acknowledgment. We gratefully acknowledge the financial support from the state National Natural Science Foundation of China (grant nos. 50325311, 50590403, 50721002) and the 973 program of the People's Repblic of China (grant no. 2004CB619002).

Supporting Information Available: X-ray crystallographic file in CIF format for the $BaTeMo_2O_9$ single crystal. This material is available free of charge via the Internet at http://pubs.acs.org.

References

(1) Harrison, W. T. A.; Dussack, L. L.; Jacobson, A. J. *Inorg. Chem.* **1994**, *33*, 6043.
(2) Harrison, W. T. A.; Dussack, L. L.; Jacobson, A. J. *J. Solid State Chem.* **1995**, *120*, 112.
(3) Harrison, W. T. A.; Dussack, L. L.; Jacobson, A. J. *J. Solid State Chem.* **1996**, *125*, 234.
(4) Balraj, V.; Vidyasagar, K. *Inorg. Chem.* **1998**, *37*, 4764.
(5) Halasyamani, P. S.; Poeppelmeier, K. R. *Chem. Mater.* **1998**, *10*, 2753.
(6) Porter, Y.; Ok, K. M.; Bhuvanesh, N. S. P.; Halasyamani, P. S. *Chem. Mater.* **2001**, *13*, 1910.
(7) Welk, M. E.; Norquist, A. J.; Arnold, F. P.; Stern, C. L.; Poeppelmeier, K. R. *Inorg. Chem.* **2002**, *41*, 5119.
(8) Goodey, J.; Broussard, J.; Halasyamani, P. S. *Chem. Mater.* **2002**, *14*, 3174.
(9) Porter, Y.; Halasyamani, P. S. *J. Solid State Chem.* **2003**, *174*, 441.
(10) Goodey, J.; Ok, K. M.; Broussard, J.; Hofmann, C.; Escobedo, F. V.; Halasyamani, P. S. *J. Solid State Chem.* **2003**, *175*, 3.
(11) Ra, H.-S.; Ok, K. M.; Halasyamani, P. S *J. Am. Chem. Soc.* **2003**, *125*, 7764.
(12) Hou, J. Y.; Huang, C. C.; Zhang, H. H.; Tu, C. Y.; Sun, R. Q.; Yang, Q. Y. *J. Mol. Struct.* **2006**, *785*, 37.
(13) Chi, E. O.; Ok, K. M.; Porter, Y.; Halasyamani, P. S. *Chem. Mater.* **2006**, *18*, 2070.
(14) Halasyamani, S. P.; Poeppelmeier, K. R. *Chem. Mater.* **1998**, *10*, 2753.
(15) Ok, K. M.; Halasyamani, S. P. *Chem. Mater.* **2006**, *18*, 3176.
(16) Oishi, S.; Teshima, K.; Kondo, H. *J. Am. Chem. Soc.* **2004**, *126*, 4768.
(17) Taylor, R.; Macrae, C. F. *Acta Crystallogr.* **2001**, *B57*, 815.
(18) Bruno, I. J.; Cole, J. C.; Edgington, P. R.; Kessler, M. K.; Macrae, C. F.; McCabe, P.; Pearson, J.; Taylor, R. *Acta Crystallogr.* **2002**, *B58*, 389.
(19) Macrae, C. F.; Edgington, P. R.; McCabe, P.; Pidcock, E.; Shields, G. P.; Taylor, R.; Towler, M.; van de Streek, J. *J. Appl. Crystallogr.* **2006**, *39*, 453.
(20) Born, M.; Wolf, E. *Principles of Optics*; Pergamon: Oxford, 1975.

CG700755P